



Effect of silver coated gear train in space vehicle under ultra-high vacuum of 10^{-7} Torr

Wonil Kwak ^{1,2}, Jeonkook Lee ², Woosub Lee ², Yongbok Lee ^{1,2,*}

¹ University of Science and Technology (UST-KIST School), 217 Gajeong-ro, Gajeong-dong, Yuseong-gu, Daejeon, SOUTH KOREA.

² Korea Institute of Science and Technology, Hwarang-ro 14-gil, Seongbuk-gu, Seoul 02792, SOUTH KOREA.

*Corresponding author: lyb@kist.re.kr

KEYWORD	ABSTRACT
Space tribology Dry friction Solid lubrication Pin-on-disk Spur gear Energy dissipation	Gear train systems used in the lunar environment should be able to endure limiting conditions such as ultra-high vacuum with minimal energy dissipation. From this point of view, we have obtained the optimum thickness of a silver coating that can influence friction mechanisms of the gear and pinion. To clarify the sliding friction between the gear and pinion, a pin-on-disk tribometer that could be implemented in space tribological applications was constructed according to the specifications of ASTM G99-95a using a solid lubricant at a vacuum pressure of approximately 10^{-7} Torr. The friction characteristics were compared for atmospheric and vacuum environments. Through these results, an improved understanding of the friction mechanisms between the gears coated with silver is obtained. Moreover, an analysis of energy dissipation due to differences in the gear backlash was conducted.

1.0 INTRODUCTION

Space applications are for the future of space activities such as building and operation of the international space station, inspection and repair of orbiting satellites, and lunar or planetary explorations (Mitsushige, 1999; Visenti and Winnendael, 2001). Space applications require enduring extreme environmental conditions such as high vacuum, gravitational fields, wide temperature gradients, solar radiation, and dust (Broscoe, 1990). In particular, the mechanical components used in space applications often suffer from friction and wear. Therefore, ensuring the reliabilities of such components is very important for a successful mission.

Received 30 June 2018; received in revised form 20 September 2018; accepted 20 September 2018.

To cite this article: Kwak et al. (2019). Effect of silver coated gear train in space vehicle under ultra-high vacuum of 10^{-7} Torr. Jurnal Tribologi 20, pp.74-86.

The challenges for future space applications will be greater because the missions are more ambitious and require more complex mechanisms to operate for longer periods of time. In the early years of the space program, the required lifetime and lifecycle of machinery were minimal, and it was usually possible to complete a successful mission in a relatively short time. As the mission lifetimes increase, the components of the machinery often break down. Thus, in the last few years, significant research has been conducted to improve these shortcomings. Further, the requirement of space robots is being considered due to the extreme environment in space.

This work aims to develop a space tribo-component that can be used in the dynamic mechanical part of the Korean Lunar Rover project. The space tribo-component will be employed to monitor dynamic factors during mission time on the lunar surface. In this paper, we describe a spur gear train for use in the rover that employs a solid lubricant.

2.0 SOLID LUBRICATION PROCESS CONSIDERATION FOR SPACE ENVIRONMENT

Many different classes of solid lubricants have been used in space applications. Soft metals that are used as solid lubricants include lead, gold, silver, and indium. Polyimides and PTFE are polymeric materials that have been previously used in space applications (Fusaro, 1990; Gardos, 1986). Solid lubricants are used to lubricate various mechanical components, such as rolling-element bearings, gears, bushings, electrical sliding contacts, seals, and robot and telescope joints.

In general, solid lubricants are used to form a thin film on a substrate that has low mechanical strength. Methods for forming the thin film include sputtering, ion plating, electroplating, and vacuum deposition. In the particular case of silver as a lubricant, the electroplating method is adopted, and the surface of a target is covered with a thin coating of silver via electrolysis. Electroplating causes the surface of the target to be mechanically hard and durable against chemical erosion.

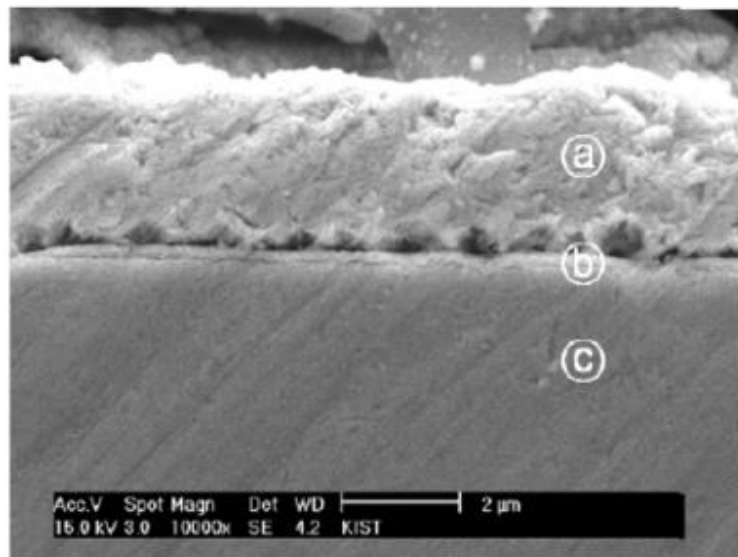


Figure 1: SEM analysis on the silver coating substrate (a) Silver (Ag) coating layer, (b) Nickel (Ni) coating layers, (c) AISI1045C, uncoated layer.

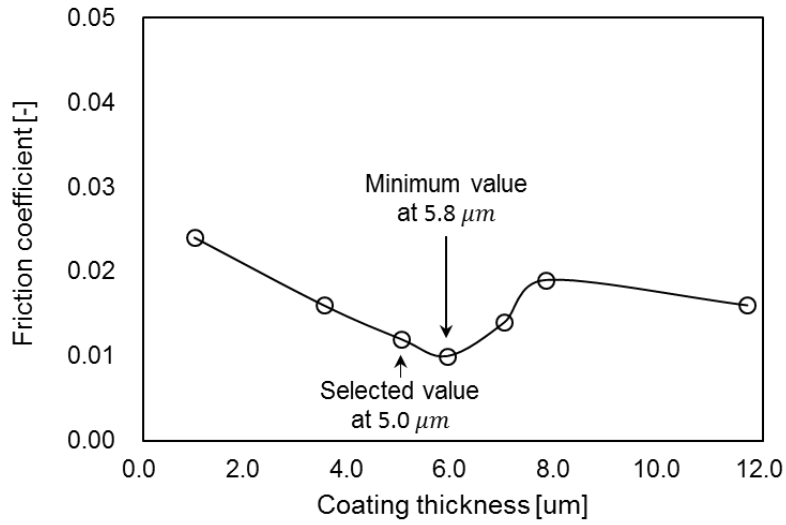
Scanning electron microscope (SEM) images of the electroplated component are shown in Figure 1. After the electroplating method for silver coating on the target. This SEM analysis shows that are not coated with any material as in (c). It also shows the layers which are confirmed that the Ni and Cu coating layers (indicate to (b)) on the upper and lower layers and also observed Ag(silver) coating layer (indicate to (a)) is applied. As the element analysis results, the materials to be coated were well coated in the proper layer. The detailed EDS analysis values are shown in Table. 1.

Table 1: EDS analysis for silver coating on the substrate plate

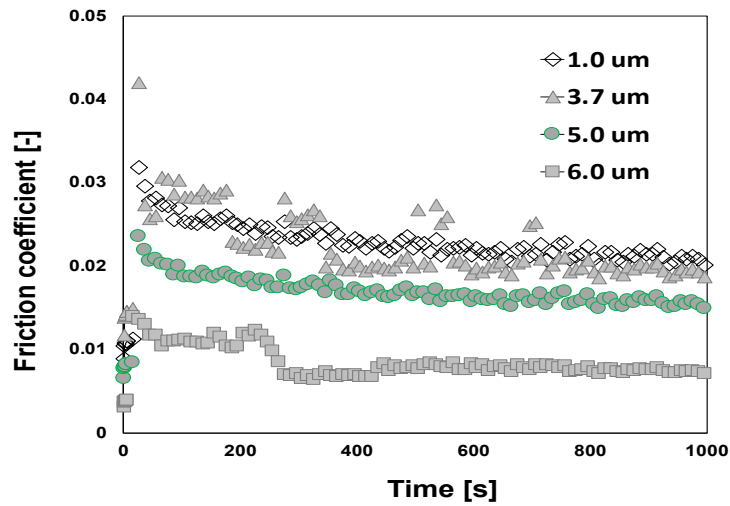
Element	(a)		(b)		(c)	
	Wt %	At %	Wt %	At %	Wt %	At %
Ag	100	100	12.04	6.08		
Cr			8.34	9.56	8.08	9.69
Fe			49.26	52.73	54.7	54.47
Ni			30.36	30.89	37.22	35.84
Total	100	100	100	100	100	100

One of the important tribological parameters is film thickness because the friction coefficient of a surface is influenced by the thickness of and contact stress created by the sliding surfaces. In the case of a soft metal such as silver, friction deformation and ploughing are possible; the coating thickness influences the friction coefficient dominantly. The solid lubricants thus need to possess the characteristics of low wear rate and high resistance to wearing. Therefore, it needs a kind of efforts as the figure 2. The optimization study for the influence of silver film thickness was conducted at Korea Institute of Science and Technology (KIST). The friction test is a type of reciprocating test, which involves the AISI1045C substrate plate tested with various silver coating thicknesses, namely, 1.0, 3.5, 5.0, 5.8, 7.0, and 8.0 μm , against the same steel block. The optimal value of the silver coating thickness is thus evaluated.

Based on the results of the aforementioned work, the thickness of the silver coating to be used on the gear for lubrication in a high-vacuum condition was formulated. However, this optimization was not enough to fully understand the effects of the silver coating on the gear train as an aspect of the tribological system. The following section describes the tribological characteristics of the silver coating on an S45C steel substrate in the ultra-high vacuum (UHV) condition.



(a)



(b)

Figure 2: Optimization of Ag (silver) coating thickness: (a) friction coefficient as a function of coating thickness, and (b) friction coefficient as a function of time for each thickness value.

3.0 PIN-ON-DISK TRIBOMETER

3.1 Experimental apparatus and test procedure

A pin-on-disk test is commonly referenced for documents on ASTM standards; therefore, this work also refers to the guidelines in ASTM G99-95a (ASTM, 2000). Although the guideline clearly provides recommendations for the test method, they are not strictly required. These

recommendations are summarized in Table 2. The recommended guidelines are not required here because it is important that the friction coefficients are individually determined according to the materials and experimental conditions. Although there has been extensive research in this field, studies on applications to components in the space environment are inadequate. Further, the wear test is an extremely sensitive experiment that is easily affected by changes in the normal force and material of the surface. Therefore, experiments are necessary to replicate the exact conditions of the lunar environment before assembling the components on the lunar rover.

Figure 3 shows the three main parts of the testing facility: main controller, data acquisition module, and vacuum chamber for the experiment. A rotary pump is sufficient to establish a vacuum pressure of approximately 10^{-3} Torr. However, realizing a UHV zone (less than 10^{-7} Torr) requires a turbo pump, and the testing facility has a turbo molecular pump (TMP).

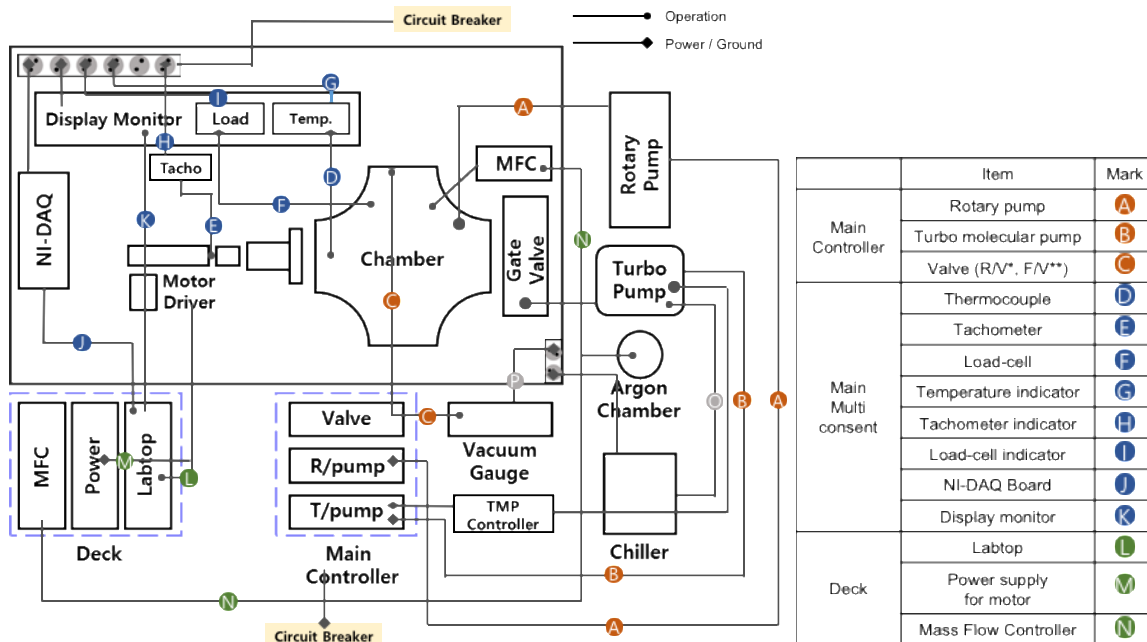


Figure 3: Ultra-high vacuum (UHV) tribology experimental apparatus.

In the present research, the pin-on-disk is used to measure load, rotating speed, and internal temperature. The components of the pin-on-disk setup are shown in Figure 4(a). A preformed surface layer was created by coating Ni on the S45C disk substrate. Subsequently, the disk was coated with the silver layer. The Ni layer helps the adhesion of silver on the surface. The Ni layer was 3–4 μm thick, and the silver coating thickness was approximately 5 μm . Thus, the total coating thickness was 8–9 μm . The disk and pin had diameters of 66 mm and 3 mm, respectively. The frictional force during the test is thus generated by the interaction between the rotating disk and the pin.

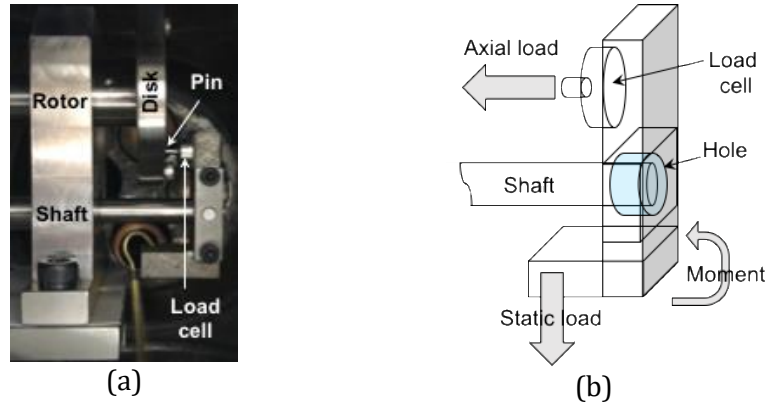


Figure 4: (a) Pin-on-disk experiment apparatus, and (b) acquisition method using an 'L' beam.

Figure 4(b) shows how to hold the pin and apply an axial-load to increase the contact pressure. The 'L' beam designed for an axial-load is used to preload the disk surface to achieve contact between disk and pin. Although this method may produce a contact angle on the load, it is negligible because the displacement of the pin by the load was very small and the results of the load measurements were constant.

The test method used here is in accordance with the guidelines of the American standard test method (ASTM), which is listed in Table 2. Therefore, this experimental condition followed the ASTM G99 standard considering a simplification of the dynamic behaviors on the gear train. The movement in this case is a pure sliding motion, which is common to many tribometers with continuous or alternative motion, and the sample was tested under the operating conditions summarized in Table 3. The samples were hardened, and the roughness on the surface was polished before coating with silver, in accordance with the standard procedures.

Although the test procedures and measurement methods have been described in several published literatures, each of those techniques was developed based on the specific experimental environment and the nature of the friction experiment; there is no universally established experimental method. This is because the friction between two objects has different characteristics depending on the individual characteristics of the contacting materials, contact conditions, measuring methods, thermal responses, operating conditions, environmental conditions, material combinations, and surface chemical compositions, among other factors. In other words, it is important to develop suitable friction test methods and test devices according to the nature of the experiment. Moreover, it is essential to verify that the friction parameters derived using the test devices are measured properly.

Table 2: Typical guidelines of ASTM G99-95a [14].

Content	Recommended range	Experimental value	Unit
Pin Specimen	Cylindrical / Spherical	Spherical Type	-
Pin Diameter	2 to 10	3	mm
Disk Diameter	30 to 100	66	mm
Disk Thickness	2 to 10	2	mm
Roughness	Less than 0.8	Less than 0.5	μm (Ra value)

Table 3: Experimental conditions of pin-on-disk test according to ASTM G99-95a.

Condition	Value	Unit
Disk Roughness	0.4	μm (Ra value)-
Vacuum Level	8×10^{-7} , 690	torr
Operating Time	1000	second
Load	0.5	N

3.2 Pin-on-disk test results and discussion for the UHV regime

Using the frictional test results, the friction coefficient was calculated as the ratio of the force signal F to axial load W . The friction coefficient μ is thus described as follows.

$$F = \mu W \tag{1}$$

The traction coefficient results were derived from experiments performed under the UHV pressure of 10^{-7} Torr and contact pressure of 0.3 GPa for the real gear train condition (when its normal load was 0.5 N). The experiments were performed at various speeds in the range of 0.2 to 3.0 m/s, and the friction coefficient was expressed as a function of the sliding velocity. At the maximum point (approximately 0.7 m/s), all plots show the same trend, increased sliding velocity, and decreased friction coefficient. These results were used to compare the friction coefficient for different slip velocities. The cases were divided into high- and low-velocity ranges for the following reasons: (1) the fitted curve for the entire range was derived according to the slip velocity to identify the frictional and wear tendencies of each material, and (2) it is important to identify the frictional tendencies over a wide range because the slip velocity decreases dramatically in space applications for operation under high-velocity conditions. Representative cases are presented in Figure 5 to illustrate the frictional tendencies at high and low velocities. For the uncoated and silver coated disk experiments, the overall friction coefficients were higher than that of the silver coated disk test. The graph below shows the curves for the effects of friction mechanisms for four cases. In this test rig, it measurement rotating speed of disk material, torque while the pin ploughed tracks on.

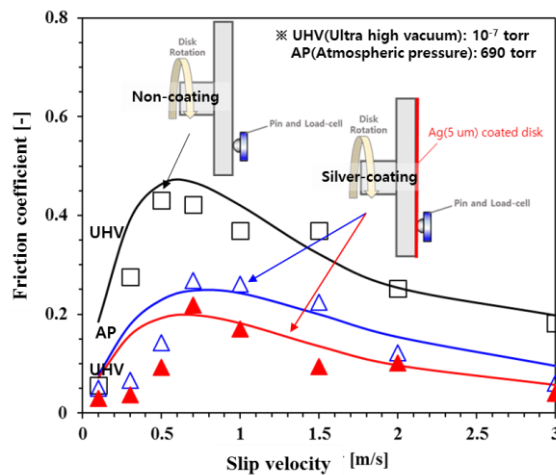


Figure 5: Friction coefficients in the UHV condition for a silver coated disk.

4.0 DYNAMIC BEHAVIOR OF THE GEAR TRAIN

4.1 Experimental apparatus and test procedure

Space robot systems contain mechanisms requiring lubrication. As the operating conditions are often demanding, the mechanics endure many challenges to ensure a successful mission. In the case of the rover, all of the dynamic mechanisms such as rover wheels, slip-ring assemblies, scanning device, robotic arms, bearings, and gear trains are component requiring lubrication (Fleishauer and Hilton, 1991). This work specifically focuses on the gear train of a lunar rover.

While the rover is on a mission, which problems affect the success of the mission? In the particular case of the gear train, the problem may depend on the detection or expectation. However, some amount of prior research is available, and it can be used to predict typical gear failure scenarios.

On the lunar surface, wearing is a phenomenon that causes critical problems in the gear train. Because of the extreme environmental condition such as UHV, directed solar radiation, and nanoparticles (lunar dust) floating on the surface, wearing is often seen on the surface of the gear tooth.

Because of wearing on the surface of the gear tooth, a gear train may lose power and experience a decrease in durability. To improve the durability and reliability of the gear train, this study examines the effect on the gear tooth design and optimization of the design parameters of the spur gear. The design parameter considered here is the addendum ratio of the gear tooth.

A commercial software for design of gear geometry and analysis of gear dynamics is used in this work. From this analysis, a specific addendum ratio is selected for the spur gear test.

For the given design parameter, the software predicts the gear dynamics; it calculates a mean friction coefficient value and friction power loss, thus predicting the reliability of the gear train. Another parameter that influences the gear dynamics is the type of lubrication used. In this study, the gear is lubricated using a solid lubricant via a silver coating.

As previously mentioned, one criterion that affects friction character is the contact stress between the friction materials. Therefore, gear dynamics of the effect of the silver coating is experimentally estimated in the vacuum chamber.

Equations (2)–(7) describe the calculation of the gear efficiency. Using some design parameters, the gear analysis software can calculate the gear dynamics. In the following equations, A describes the distance between the middle line of the pinion to the gear assuming ideal geometry, Z_1 and Z_2 are the number of teeth on the gears, and m is a module of the gear train.

Further, A_f is the center displacement of the machining gear, D_1 and D_2 are the diameters of the pitch circles of the pinion and gear, and Y is an increment factor of the center displacement. If the gear experiences backlash, its center displacement is calculated by A_c . Finally, the backlash of the gear train is calculated using Equation (7) to obtain C_0 .

$$A = \left(\frac{Z_1 + Z_2}{2} \right) m \quad (2)$$

$$A_f = \left(\frac{D_1 + D_2}{2 \cos \alpha} \right) \quad (3)$$

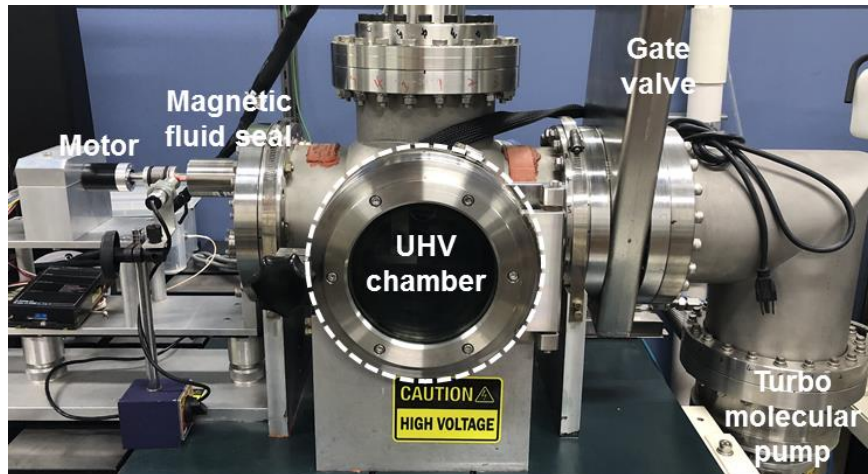
$$y = \left(\frac{A_f - A}{m} \right) \quad (4)$$

$$A_c = \frac{B_f}{2 \sin \alpha} \quad (5)$$

$$A_f = A + ym + A_c \quad (6)$$

$$C_0 = \frac{2\Delta \sin \alpha - \Delta S1 - \Delta S2}{\cos \alpha} \quad (7)$$

This space tribocomponent experiment apparatus could thus be used to measure the dynamics of the gear and bearings in a high vacuum chamber. The chamber is 8-inch standard 6 ways cross. One way of bottom is a blank cover. Measurements of the rotating speed of the pinion, torque, and displacement between the gear train can be obtained in real-time. The widths of the gear and pinion are 8 mm each, and the gears have the standard module (module is 1.0) in this study. This test rig is a preliminary setup for verifying the measurement system in real-time; however, the advanced test rig would be of a suitable size for the Korean lunar rover. The environmental condition in the chamber is set as UHV of 10^{-7} Torr. Therefore, using this test chamber, it is possible to investigate the effectiveness of the solid lubricant in high vacuum. Two eddy current sensors measure displacements between the gears, which can be used to calculate backlash in real-time.



(a)

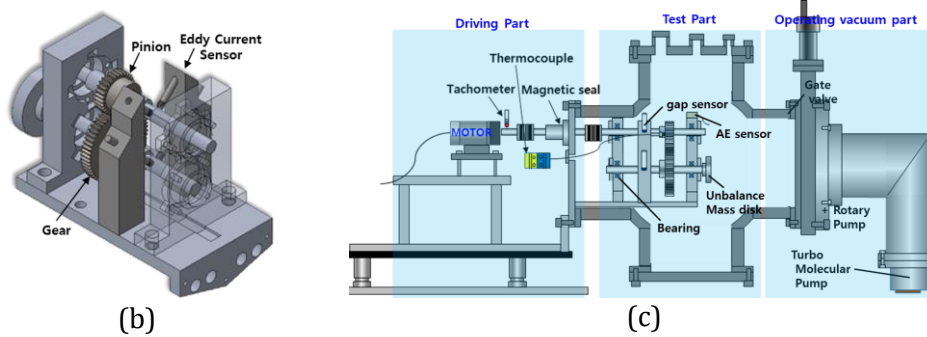


Figure 6: Ultra-high vacuum (UHV) tribology experimental apparatus (a) General view; (b) spur gear experimental segment—upper gear means a pinion and below gear is named a gear; (c) cross-sectional view of the gear train system in the UHV chamber: it consists of pinion, gear, gap sensors, and tachometer

4.2 Gear train test results and discussion for the UHV regime

Comparing differences due to rotating speeds of 80 and 180 rpm, backlash variation can be ignored. However, in this experiment, the measured error is comparable to ideal backlash. Thus, this measurement system can be used to obtain a more specific prediction for gear power loss when the space rover is involved in real-time missions. Figure 7 shows the orbital displacements of the pinion and gear at a pinion rotating speed of 180 rpm. The other pair graph shows the orbital displacement when the pinion rotating speed was 80 rpm. Thus, the gear train has a gear module ratio of one sixth (1/6).

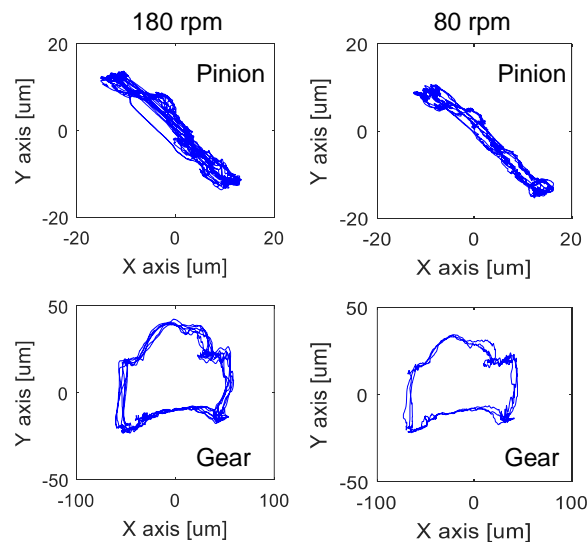


Figure 7: Spur gear experiment results for the orbital displacement of gear shaft indicating operating stability.

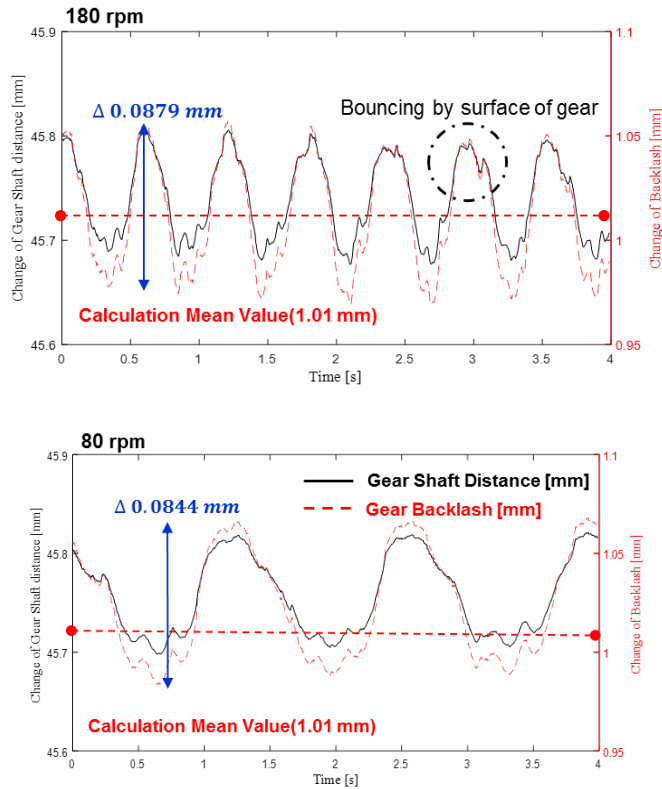


Figure 8: Spur gear experiment results indicating the backlash due to differences in the rotating speeds.

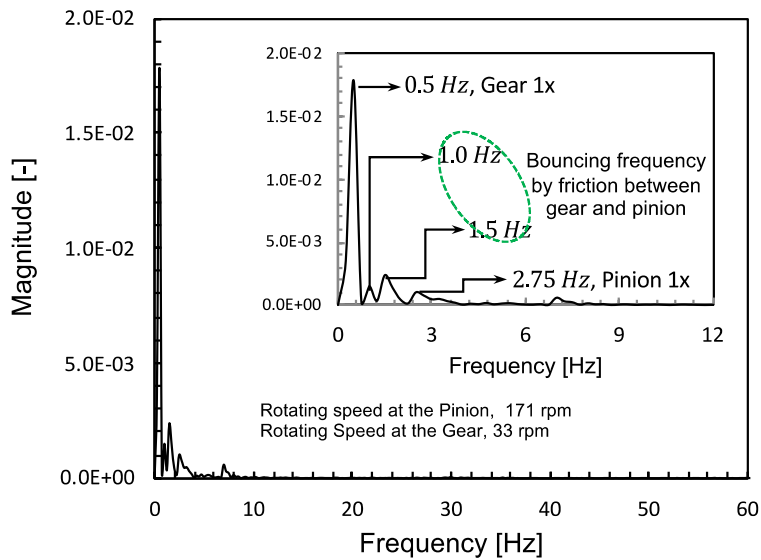


Figure 9: Fast Fourier Transform (FFT) analysis using the vibration signals of the gear shaft.

Figure 9 shows the results of the fast Fourier transform analysis for specific peaks in the frequency domain. At the analysis point, the motor speed was 180 rpm; however, the pinion rotating speed was approximately 171 rpm and gear rotating speed was approximately 33 rpm. Consequently, some peaks are observed at 0.5 Hz and 2.75 Hz. However, other peaks have more scientific significance than peaks related to the operating speed. Peaks were seen for the bouncing vibration of the friction mechanism between the contact areas during operation of the gear. It can be seen from Figure 9 that the bouncing due to friction of the gear surface appears as high frequency components, and a simple high pass filter could be used to extract this information from the frequency response.

5.0 CONCLUSION

In this study, the authors have applied and verified a modified version of the pin-on-disk and gear train test to understand the real frictional processes in a gear train with silver coating as a solid lubricant and different sliding velocities. The test reveals the two stages of the friction process and the friction coefficient tendency appropriate to the studied pin-on-disk test under different sliding velocity conditions. It was observed that the friction coefficient decreased when sliding velocity increased in the UHV condition of 10^{-7} Torr.

Considering the correlations between the friction mechanisms and the backlash of the gear train, the differences between the calculated and experimental results may be considered as loss due to energy dissipation to indicate whether the friction originates from the tooth area or the deterioration area. The test also provides information on selecting the appropriate materials for space applications or to adjust the application conditions to allow the best performance for a given material. This is a quick method to quantify the peaks from the frequency analysis as indicators of not only differences in backlash fluctuation but also working conditions beyond those of the standardized testing cases of G99, as demonstrated in the present study.

For edification on the use of the multi-pass dual-indenter method in the variant proposed in this work, additional investigations are needed to elucidate the influences of energy dissipation and wear mechanisms as well as those related to the surface morphology of the tested gears. An approach to this line of investigation will be attempted in the UHV testing facility with the silver coated gear train.

ACKNOWLEDGEMENT

This research was supported by the MSIP under the space technology development program (NRF-2016M1A3A9005563) supervised by the NRF. Additionally, this material is based on research projects ("Reliability of ball bearing for extreme environment and development of smart ball bearing core technology" NRF-2017R1A2A1A17069515) supported by the National Research Foundation of Korea, which is funded by the Ministry of Science, ICT, and Future Planning, Korea. The authors would like to thank the researchers of this project for their contribution to the study.

REFERENCES

- Broscoe, H. M. (1990). Why space tribology. *Tribology International*, 23, 67-74.
- Development of the prototyping ball bearings for a rocket turbopump. (2014). Korea Institute of Science and Technology.
- Fleishauer, P. D., & Hilton, M. R. (1991). Assessment of the tribological requirements of advanced spacecraft mechanisms, Report no. TOF-0090(5064)-1, Aerospace Corporation.
- Fusaro, R. L. (1990). Self-lubrication polymer composites and polymer transfer film lubrication for space applications. *Tribology International*, 23, 105-122.
- Fusaro, R. L. (1994). Lubrication of space systems. NASA Technical Memorandum 106392, pp. 1-28.
- Gardos, M. N. (1986). Self-lubrication composites for extreme lubricating conditions, friction and wear of polymer composites (Klaus ED. F.). Elsevier Science Publishers.
- Gupta, P. K. (1984). *Advanced dynamics of rolling elements*. Springer.
- Jones, W. R., & Jansen, M. J. (2005). Lubrication for space applications. National Aeronautics and Space Administration, Final contraction report.
- Korean lunar exploration project. (2014). Korea Institute of Science and Technology.
- Mitsushige, O. (1999). Space robot experiments on NASA's ETS-VII satellite. *IEEE International Conference on Robotics & Automation*, pp. 1390-1395.
- Miyoshi, K. (1999). Considerations in vacuum tribology (adhesion, friction, wear and solid lubrication in vacuum). *Tribology International*, 32, 605-616.
- Nomenclature of gear tooth failure modes, AGMA 110.04:1980.
- Standard test method for wear testing with a pin-on-disk apparatus. (2000). ASTM, pp. 1-6.
- Townsend, D. P., & Akin, L. S. (1980). Analytical and experimental spur gear tooth temperature as affected by operating variables. 3rd ASME Conference, *Journal of Mechanical Design*, pp. 25-30.
- Visenti, G., Winnendael, M., & Putz, P. (2001). Advanced mechatronics in ESA's space robotics developments. *IEEU/ASME International Conference on Advanced Intelligent Mechatronics Proceedings*, pp. 1261-1266.
- Zaresky, E. V. (1990). Liquid lubrication in space. *Tribology International*, 23, 75-93.